Int. J. Heat Mass Transfer. Vol. 35, No. 9, pp. 2233–2244, 1992
Printed in Great Britain

0017–9310/92 $5.00 + 0.00

Scalar rate correlation at a turbulent liquid free surface: a two-regime correlation for high Schmidt numbers

BOO-CHEONG KHOO† and AIN A. SONIN
Department of Mechanical Engineering, Massachusetts Institute of Technology, Cambridge, MA 02139, U.S.A.

(*Received* 15 *October* 1990 *and in final form* 12 *August* 1991)

Abstract—An experimental correlation is derived for gas absorption at a turbulent, shear-free liquid interface. The correlation is expressed in terms of the liquid-side turbulence intensity, liquid-side macroscale, and the properties of the diffusing gas and solvent. The transfer coefficient increases linearly with r.m.s. velocity up to a point where the eddy Reynolds number reaches a critical (Schmidt number dependent) value. At higher velocities, there is a more rapid linear rise. The slope of the lower Reynolds number region is proportional to the square root of the diffusivity; at Reynolds numbers much higher than that of the break point, the slope becomes independent of diffusivity.

1. INTRODUCTION

SINCE the early work of Lewis and Whitman [1] and Higbie [2], a considerable body of literature has been built up on gas absorption at a turbulent liquid interface. It is fair to say, however, that even now our understanding of this problem is much more primitive than, for example, that of turbulent transport at a solid surface. There is no concensus on a universal model, or even on a single empirical correlation, for the free-surface transport problem (e.g. see the reviews by Sonin *et al.* [3] and Theofanous *et al.* [4], as well as contributions in the monograph by Brutsaert and Jirka [5]).

The present work attempts to derive an empirical correlation for high Schmidt number mass transfer at a shear-free, turbulent liquid interface, under conditions where transport on the liquid side is rate-limiting. Our purpose is to present a correlation in terms of fluid properties and parameters which characterize the local interfacial liquid-side turbulence. The hope is that this will yield a correlation that can be applied generally to shear-free interfaces of turbulent liquids, independent of the precise way the turbulence in the liquid is generated, and guide us towards a more general model for the transport process.

The experiments were done in a previously developed apparatus [3, 6] in which easily controlled, steady turbulence can be imposed from below on a shear-free liquid interface. This system has already been used to obtain a correlation for the condensation of pure vapor at a turbulent liquid interface [6], which is basically a moderate Prandtl number liquid-side heat transfer problem. In the absence of buoyancy effects, the transport coefficient was found to be linearly dependent on the r.m.s. value of the fluctuating velocity on the liquid side and proportional to the inverse one-third power of the bulk liquid Prandtl number, at least in the low Prandtl number range investigated ($1 < Pr < 6$). The present work addresses the analogous mass transfer problem at high Schmidt numbers in the range 230–1600.

2. APPARATUS AND GAS ABSORPTION MEASUREMENT

Sonin *et al.* [3] have shown that a vertical, axisymmetric confined jet in a cylinder partially filled with water induces a bulk-flow-free and reasonably uniform turbulence in the region located away from the damped layer at the interface and at distances greater than 3D from the nozzle, D being the diameter of the cylinder. The turbulence decays with elevation from the nozzle and is relatively isotropic in a horizontal plane. The turbulence intensity in the water can be easily controlled by varying the momentum flux through the nozzle and the water level in the test cell. The system also possessed an integral length scale at height $z > 3D$, which is locked to the tube diameter [3, 6]. This is a distinct advantage: simply by changing the tube size, we can have turbulence with different integral length scales. This could be aptly used in the characterization of the turbulence structure close to the interface, which ultimately controls the transport process across it.

Our apparatus was similar in design to that used in ref. [3]. It consisted of a vertical, axisymmetric nozzle

† Present address: Dept. of Mechanical & Production Engineering, National University of Singapore, 10 Kent Ridge Crescent, Singapore 0511.

NOMENCLATURE

A	gas–liquid interfacial area [m^2]
C	species concentration [mol m^{-3}]
C_s	saturated concentration of the gas in the liquid [mol m^{-3}]
d	nozzle exit diameter, Fig. 1 [m]
D	test cell inside diameter, Fig. 1 [m]
D	molecular diffusivity of the gas in the liquid [m^2 s^{-1}]
K_L	mass transfer coefficient across the interface [m s^{-1}]
K_*	mass transfer coefficient corresponding to the 'break' velocity as defined in equation (13) [m s^{-1}]
Pr	Prandtl number
Q	volumetric flow rate circulating through system, Fig. 1 [m^3 s^{-1}]
r	radial coordinate measured from the cylinder axis [m]
$R(t)$	Eulerian autocorrelation function measured at a fixed point, equation (8)
Re	Reynolds number, $v\Lambda/\nu$
Re_s	system Reynolds number, $Q/d\nu$
Re_*	break Reynolds number, $v_*\Lambda/\nu$, equation (13)
Sc	Schmidt number, ν/D
St	Stanton number, K_L/v
v	r.m.s. velocity of either the horizontal or vertical component of turbulent velocity [m s^{-1}] at the 'interface' obtained by extrapolating from the bulk, disregarding surface damping
v_*	value of v at the 'break' point, as defined in equation (13)
z	vertical coordinate measured upwards from the nozzle [m].

Greek symbols

Λ	integral length scale of turbulence eddies as defined in equation (6) [m]
ν	liquid kinematic viscosity [m^2 s^{-1}]
τ	characteristic time as defined in equation (7) [s]
$\Phi(Re_s)$	function defined in equations (4) and (5).

Subscript

*	refers to the 'break' point.

placed in a pyrex tube partially filled with water, as shown in Fig. 1. A centrifugal pump circulated the water through a closed loop system, with the temperature controlled by a heat exchanger. The total volume in the system was deliberately kept to a minimum to minimize the time required for each gas absorption experiment. (As in any gas absorption experiment, the amount of dissolved CO_2 in the system reached a readily measurable quantity only after a fairly long time.) Two different test cell diameters D were used, 0.152 and 0.038 m. The respective nozzles had diameters d of 0.0064 and 0.0016 m, giving a ratio of D/d as 24, similar to that used in refs. [3, 6].

CO_2, which was used in all the gas absorption measurements, was introduced just above the interface and exhausted at a higher station. Our aim was to prevent any build up of noncondensable gases, notably air, residing next to the interface. Air, being lighter than CO_2, would naturally tend to be exhausted out of the system. In order to ensure that the CO_2 coming into the test section did not induce 'extra' turbulence at the interface, a large inlet tube was used to reduce inflow velocity. With the pump shut off, the interface remained perfectly still before and after the valve controlling the supply of CO_2 was turned off. Also, the incoming CO_2 was preheated by passing the gas through a copper tubing, immersed in a water–

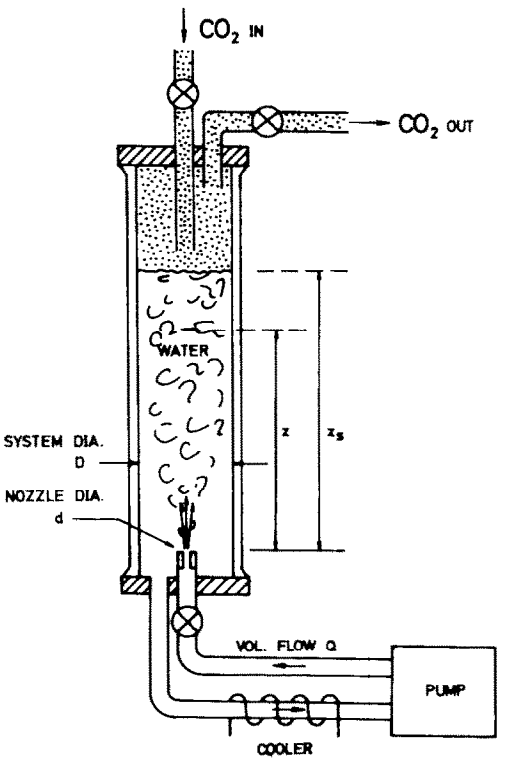

FIG. 1. Schematic of test cell.

glycerol mixture bath so that it was at the same temperature as the bulk water in the test section. In this way, we were able to maintain a gas temperature within ± 0.5°C of the water temperature, thereby ensuring a known gas temperature at the interface, which was important since the saturated concentration of CO_2 in water is highly dependent on temperature (there is a variation of about 3% for every degree Celsius change in temperature). The saturation concentration of CO_2 was computed based on the work of refs. [7–9].

In each test, the system was first allowed to run for at least 20 min with CO_2 inflow to reach the desired steady-state operating condition. Five different samples (50 ml) of the bulk water were taken to determine the initial average concentration of dissolved CO_2. The water level in the test cell was then reduced precisely to the desired z_s/D level, z_s being the height of the interface above the inlet nozzle. The system was restarted and run for a time ranging from 5 to 12 h, depending on the turbulence intensity imposed. At the end of the run, seven samples were taken for determining the average final concentration. The amount of dissolved CO_2 in the samples was determined using an Orion Research carbon dioxide electrode (model 95-02) which has an accuracy of $\pm 5\%$. The electrode was initially calibrated against samples (supplied by Orion Research) of known value of dissolved CO_2 in the solution, and at 2 h intervals as recommended.

The governing equation for the transfer of CO_2 into the liquid volume of the test system is given by

$$V\,\mathrm{d}C/\mathrm{d}t = K_L A(C_s - C) \tag{1}$$

where V is the volume of water in the system, A is the area of the interface, C is the bulk concentration of CO_2 in water, C_s is the saturated concentration of CO_2 at the interface, K_L is the mass transfer coefficient [m s^{-1}] and t is the time in seconds. Under steady-state operating conditions, equation (1) can be integrated to give

$$K_L = V/At \ln((C_s - C_i)/(C_s - C_f)) \tag{2}$$

where C_i is the initial concentration of CO_2, C_f is the final concentration of CO_2 and t is the time duration of the run. With C_i and C_f measured, equation (2) gives the mass transfer coefficient K_L. After each run, the system was flushed thoroughly with tap water before a new run was initiated.

3. TURBULENCE CHARACTERISTICS

3.1. *R.m.s. velocity correlation*

Sonin *et al.* [3] have shown, using scaling arguments, that in the jet's far field, i.e. at elevations z sufficiently far above the nozzle exit (but not too close to the interfacial damped layer), the r.m.s. value of a fluctuating component of velocity v obeys the relation,

$$v(r, z) = (Q/\mathrm{D}d) f(Re_s, r/\mathrm{D}, z/\mathrm{D}). \tag{3}$$

Here, Q is the liquid volume flow rate circulating through the system, Re_s ($\equiv Q/dv$) is the system Reynolds number based on the characteristic speed through the nozzle $Q/\mathrm{D}d$, the system diameter D and the liquid kinematic viscosity v, and r is the radial coordinate. Both their experimental data and the subsequent data of Brown *et al.* [6] further suggested that, for $3.1 < z/\mathrm{D} < 4.2$, the centerline v has the form,

$$v(0, z) \simeq \Phi(Re_s)(Q/\mathrm{D}d)\,\mathrm{e}^{-1.2z/\mathrm{D}}. \tag{4}$$

Here, v can be interpreted as the r.m.s. value of *either* the axial or the radial fluctuating velocity component *at the centerline* (recall that the turbulence below the surface layer is isotropic in the horizontal plane). The function $\Phi(Re_s)$ is reproduced in Fig. 2. As discussed in ref. [6], there is some ambiguity as to the exact form of $\Phi(Re_s)$ since there is considerable scatter in the data, especially among those data points obtained using the high speed video camera system rather than the LDV (Laser Doppler Velocimeter). Instead of setting $\Phi(Re_s) = 23.4$, which is the overall average, we shall use in what follows

$$\begin{aligned} \Phi(Re_s) &= 24.5 \quad Re_s < 15\,000 \\ &= 21.8 \quad Re_s > 30\,000 \end{aligned} \tag{5}$$

which are the average values in their respective Re_s ranges. This is done so that $\Phi(Re_s) = 21.8$ reflects more closely the data obtained using the LDV, where the sample size of 10 000 is clearly a better statistical representation compared to the sample size of between 60 and 200 in the other data collected using the high speed video camera. Also, for $Re_s < 15\,000$, the data tend to scatter more above the overall mean. Clearly, the issue about the exact form of $\Phi(Re_s)$ can only be resolved when more data are collected, especially in the 'intermediate' Re_s range of between 15 000 and 30 000, where there is an absence of data. For more details about the velocity measurements, refer to refs. [6, 10].

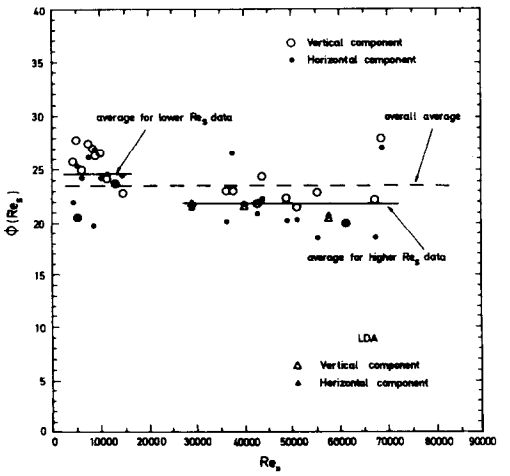

FIG. 2. Calibration of turbulence intensity at centerline of test cell.

3.2. *Macroscale*

The macroscale of the system was defined in Brown *et al.* [6] as

$$\Lambda = (v\tau)_{r=0} \tag{6}$$

where τ is a characteristic time,

$$\tau = \int_0^\infty R(t)\,\mathrm{d}t \tag{7}$$

and

$$R(t) = \langle v'(t+t')v'(t')\rangle / v^2 \tag{8}$$

is the Eulerian autocorrelation measured at the centerline, v' is either the vertical or horizontal component of the fluctuating velocity, v is the r.m.s. value of the same component, and the symbol $\langle\cdot\rangle$ represents ensemble average. Brown *et al.* found that Λ was essentially invariant for a range of v and could be approximated by the expression

$$\Lambda \simeq 0.24\mathrm{D} \tag{9}$$

where D is the test cell diameter.

We shall use v and Λ to characterize the turbulence at the liquid-side, close to the interface. In what follows, v denotes the r.m.s. value of *either the vertical or horizontal (radial) fluctuating velocity component at the centerline, extrapolated from the bulk region (where it decays with z) to the interface.* The dimensionless group associated with it is the eddy Reynolds number,

$$Re = v\Lambda/\nu. \tag{10}$$

It should be noted, however, that the use of a single r.m.s. velocity for turbulence characterization implicitly assumed that it is the single most important parameter governing the transport rate across the interface. From the LDA measurement of the velocity distribution at depths closer to the interface within the damped layer [6], both the horizontal and vertical r.m.s. velocities deviate from the behavior given in equation (4), with the vertical fluctuations being damped and their kinetic energy imparted to the velocity components parallel to the surface. While the exact spatial variation of the turbulence directly beneath the surface might have some bearing on the transport rate, we have assumed its effect to be secondary. A more sophisticated characterization of turbulence, on the other hand, will definitely incorporate more parameters and require detailed measurements of the turbulence field, especially close to the interface. Experimental measurement of turbulence distribution near a free surface is very limited, and those available used conventional instruments like the hot-wire anemometer or LDA, which are not capable of tracking the fluctuating interface and thus unable to determine the *exact* distribution with respect to the surface. The recently available PIV (particle image velocimetry) seems to be the ideal choice, capable of tracking both the interface and the velocity field beneath it simultaneously and one of us (B.C.K.) is currently working on the subject.

Table 1. Operating conditions of the experiment

Bulk water temperature (°C)	40	29	23	25†
$\nu \times 10^6$ ($m^2\,s^{-1}$)	0.6529	0.8148	0.9325	1.840
$D \times 10^9$ ($m^2\,s^{-1}$)	2.8	2.18	1.78	1.13
Sc	230	377	525	1600
$C_{sat} \times 10^2$ (mol l^{-1})	2.407	3.120	3.640	2.630

ν is the kinematic viscosity of the bulk water, D is the diffusivity of CO_2 in the liquid and C_{sat} is the saturation condition of CO_2 in the liquid.

† Water mixed with 21% by volume of glycerol.

4. RESULTS AND DISCUSSION

All the gas absorption experiments were performed using CO_2 as the transfer agent, and operating under four different Schmidt numbers (*Sc*) of 230, 377, 525 and 1600. The lower three Schmidt numbers were obtained by operating at bulk water temperatures of 40°C, 29°C and 23°C respectively. To achieve $Sc = 1600$, a mixture of water and glycerol (21% by volume) at 25°C was used as the solvent. The operating conditions are tabulated in Table 1. For each *Sc*, data were obtained for a range of turbulence intensities.

Results for the mass transfer coefficient K_L vs v are plotted in Figs. 3–6. All these plots have common features: there appears to be linear rise in K_L from the origin and then a fairly abrupt 'break' which is followed by another linear rise with much higher slope. Most previous researchers have not noted such a break, and have used a power law (or polynomial function) to fit all their data. A distinct break has, however, been noted by some investigators in cases where the surface turbulence is generated by a strong wind blowing above the interface, i.e. by interfacial shear (e.g. see refs. [11–13]). It is generally postulated

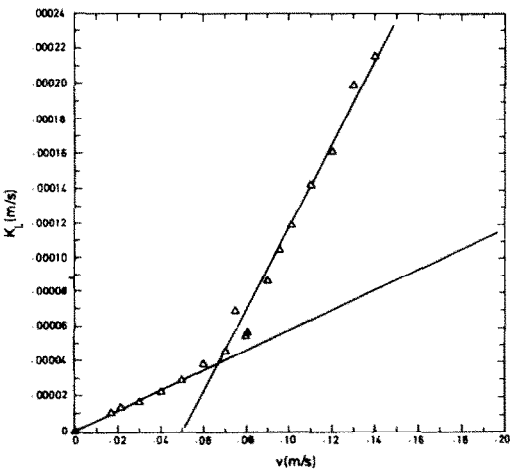

FIG. 3. Mass transfer coefficient, K_L (m s^{-1}), vs turbulence intensity, v (m s^{-1}), at $Sc = 230$.

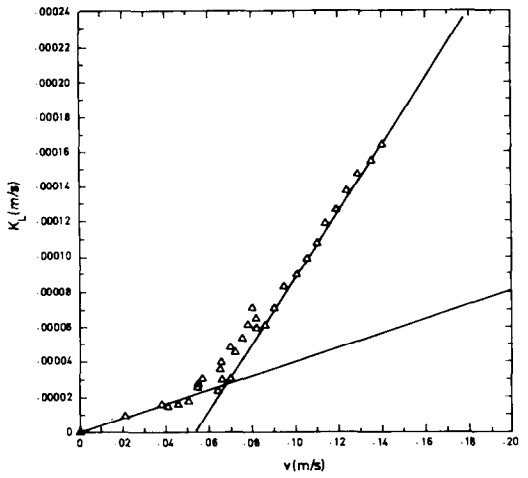

FIG. 4. Mass transfer coefficient, K_L (m s^{-1}), vs turbulence intensity, v (m s^{-1}), at $Sc = 377$.

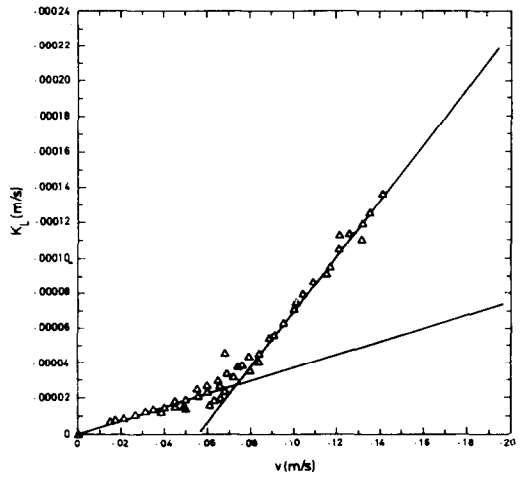

FIG. 5. Mass transfer coefficient, K_L (m s^{-1}), vs turbulence intensity, v (m s^{-1}), at $Sc = 525$.

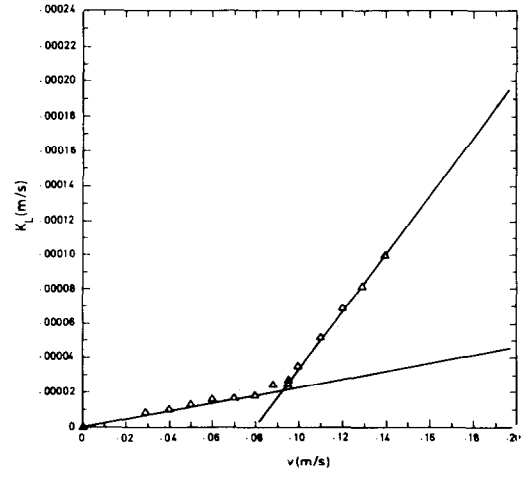

FIG. 6. Mass transfer coefficient, K_L (m s^{-1}), vs turbulence intensity, v (m s^{-1}), at $Sc = 1600$.

that this latter break occurs because of the onset of wave breaking, which causes gas bubbles to be entrained into the liquid and increases the effective surface associated with the absorption process. It should be noted, however, that the break point in our data is definitely *not* related to any wave breaking or gas bubble phenomena. In all our experiments, the liquid interface did not fluctuate more than 1–2 mm in amplitude, and no bubbles were observed on the liquid side.

If v_* is the r.m.s. velocity corresponding to the break point, we expect that

$$v_* = v_*(D, \rho, \nu, \Lambda) \tag{11}$$

where D is the molecular diffusivity, ρ is the density of the liquid, ν is the kinematic viscosity of the liquid and Λ is the macroscale as defined in equation (9). It follows that a break Reynolds number, $Re_* (\equiv v_*\Lambda/\nu)$, must be a function of only the Schmidt number, i.e.

$$Re_* = v_*\Lambda/\nu = f(Sc). \tag{12}$$

This scaling relation suggests that the 'break' velocity should be inversely proportional to the macroscale Λ if Sc is held constant. In order to check this conclusion, we carried out a series of mass transfer experiments at a bulk water temperature of 23°C (i.e. $Sc = 525$) in a smaller test cell with diameter D = 0.038 m, four times smaller than the former system. Using the empirical relationship (9), the macroscale Λ_2 associated with the smaller test cell would be four times smaller than the macroscale Λ_1 (0.037 m) associated with the larger system. Equation (12) implies that the break velocity $(v_*)_2$ associated with the smaller system should be four times larger than the corresponding break velocity of the larger system at the same Sc of 525.

Figure 7 shows the plot of K_L vs v for D = 0.038 m. The relationship is linear, and passes through the break velocity of the large system, $v_* = 0.073$ m s^{-1},

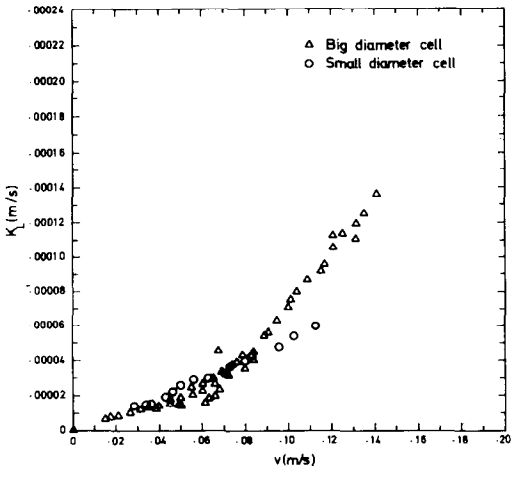

FIG. 7. Mass transfer coefficient, K_L (m s^{-1}), vs turbulence intensity, v (m s^{-1}), for test cells with D = 0.038 m (small) and 0.152 m (big) at $Sc = 525$.

Table 2. Conditions at the 'break' point

Sc	230	377	525	1600
v_* (m s^{-1}), break velocity	0.066	0.068	0.073	0.092
Re_*, break Reynolds number	3851	3180	2983	1905
$Re_* Sc^{0.4}$	33900	34100	36500	36400
Average $(Re_A)_* Sc^{0.4} \simeq 3.5 \times 10^4$				

without a break. Our scaling analysis thus appears to be confirmed. We were not able to obtain data for the smaller system at or beyond its break velocity because the interface became very wavy before such high velocities could be reached. The presence of waves would have required the inclusion of more parameters for the calibration of turbulence on the liquid side, not to mention the need to estimate the average wavy interfacial area required for computing K_L. Throughout *all* our experiments, we deliberately kept the turbulence intensity at levels where the surface wave amplitudes were below a few millimeters.

With data from the four tests with different Sc, we can try to establish the function $f(Sc)$ in equation (12) empirically. The data suggest (Table 2) that the break point Reynolds number can be approximated by

$$Re_* \simeq 3.5 \times 10^4 \, Sc^{0.4} \quad \text{for} \quad 230 < Sc < 1600 \tag{13}$$

where the break point (denoted by *) is defined as the intersection point of the two linear regions (see Figs. 3–6). Although equation (13) is derived for the indicated range of high Sc, we obtain some idea of whether it might also apply at much lower Sc by referring to the data of Sonin *et al.* [3] and Brown *et al.* [6] for condensation heat transfer at Prandtl numbers in the range 1.5–6.0. Their vapor condensation data, obtained using identical systems, showed a linear relation (at least at zero Richardson number in the case of ref. [6]) between K_L and v, with *no* break point, for r.m.s. velocities as large as 0.15 m s^{-1}. This result is at least consistent with equation (13), which predicts that at $Sc = 10$, say, the break Reynolds number is 1.4×10^4, which is much higher than the maximum Reynolds number in the experiments described by refs. [3, 6].

One conceivable explanation for the 'break' observed in our data is that our interfaces were contaminated with monolayers of surfactant or even dust. The break point might then signal the condition where the turbulent intensity becomes strong enough to actually break up the surface contamination. Contamination might conceivably have arisen, for example, from oil leakage from the pump. Davies and co-workers [14] have done extensive work on gas absorption through monolayers and found that monolayer resistance can cause mass transfer rate reductions of as much as 50%, depending on the liquid-side turbulence intensity and the amount and type of surface contamination. Davies *et al.* [15] postulated that a monolayer acts not only as a direct physical barrier to transport at the interface, but also offers 'hydrodynamics resistance' by damping out the eddies in the vicinity of the interface, thereby causing a reduction in the transport rate compared with the clean surface condition. Their experimental data showed that the greatest reduction in transport rate occurred when the turbulence intensity in the liquid was fairly low, which suggested that the cause was the inability of the surface-clearing eddies to break up the surface film. Above a certain turbulence intensity, the corresponding percentage reduction in K_L became smaller. At very high turbulence intensity, the effect of the monolayer was reduced to the layer's resistance (physical barrier) to transport. They found that the effect of even a small amount of active contamination, of order 1 p.p.m., was measurable for some contaminants.

In view of this, we carried out a series of experiments designed to check if there was any change in surface tension before and after the mass transfer experiment (monolayers generally alter the surface tension). Care was taken to test only water taken from very near the interface. Our Cenco tensiometer registered at most a ± 0.0001 N m^{-1} variation in the surface tension of the water, which was measured as 0.0728 N m^{-1} (20°C) irrespective of time or the test conditions. Orridge [16] has studied the effect of 0.1 p.p.m. of sodium sulfsuccinate as surfactant on the flow down an inclined plane. He registered a 15% reduction in CO_2 transfer rate with an accompanying 0.0011 N m^{-1} decrease in surface tension. Our maximum ± 0.0001 N m^{-1} variation in surface tension thus suggests that surfactants were absent or insignificant in our tests. Orridge's result also showed a maximum reduction of 50% in the transport rate when the surfactants were increased to 10 p.p.m., with an accompanying decrease in surface tension of 0.009 N m^{-1}. Typically, the slope dK_L/dv increases in our experiment by a much greater factor—at least 4—as the break point is traversed. This also suggests that monolayer contamination is most likely ruled out as the reason for the 'break' in our data.

By using a scaling argument similar to that of Sonin *et al.* [3], we can establish, in the simplest case where the liquid-side turbulence 'at' the surface is characterized by v, ρ, ν and Λ, that

$$St = St(Re, Sc) \tag{14}$$

where St is the mass transfer Stanton number,

$$St = K_L/v = j/v\Delta C. \tag{15}$$

Here j is the molar flux transport across the interface and ΔC is the molar concentration difference between the liquid surface and the liquid bulk. At velocities below the break velocity, our data show that K_L/v is constant, which implies that St is independent of Re.

Table 3. St vs Sc for $Re < Re_*$

Sc	230	377	525	1600
$St = dK_L/dV$	0.00060	0.000433	0.00040	0.00025
$St\,Sc^{0.5}$	0.0091	0.0084	0.00916	0.0101

Average $St\,Sc^{0.5} \simeq 0.0092$

Most models developed for interfacial transport (prominent examples are the large-eddy model of Fortescue and Pearson [17] and the small-eddy model of Lamont and Scott [18]; for a review of the various models, see Sonin *et al.* [3]) suggest that the Stanton number is proportional to the -0.5 power of Sc, i.e.

$$St \propto Sc^{-0.5}. \tag{16}$$

Table 3 gives the Stanton number or slope dK_L/dv, for $Re < Re_*$. The data can be correlated well with

$$St\,Sc^{0.5} \approx 0.0092 \pm 0.0018 \quad (Re < Re_*). \tag{17}$$

A nondimensional plot of $St\,Sc^{0.5}$ vs Re (Fig. 8) indicates the approximately constant region of about 0.0092.

For the 'post-break' region $v > v_*$, we plot $(K_L - K_*)/(v - v_*)$ against Re in Fig. 9, excluding those data very close to the break region, as any slight scatter of the data in that region would make its effect felt disproportionately due to the denominator, $v - v_*$. v_* is defined by equation (13), and K_* by equations (13) and (17). The results of Fig. 9 suggest that for $v > v_*$, the slope $(K_L - K_*)/(v - v_*)$ is approximately constant, or at most a weak function of Re and Sc. For the 'post-break' region, we can write, approximately,

$$(K_L - K_*)/(v - v_*) \simeq 0.0020 \pm 0.0003 \quad (Re > Re_*). \tag{18}$$

The only model proposed to date which suggests that St is independent of Sc is the one of Kishinevsky [19].

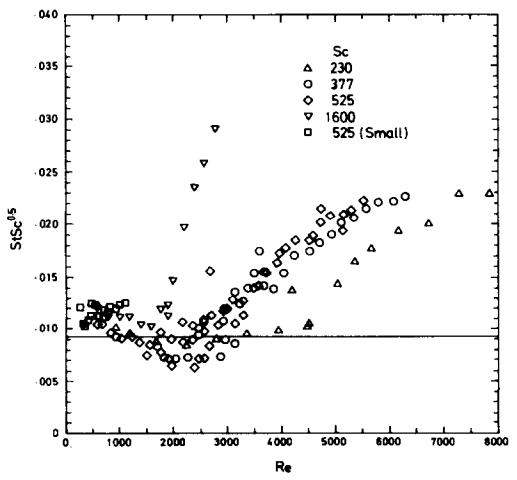

FIG. 8. $St\,Sc^{0.5}$ vs Re.

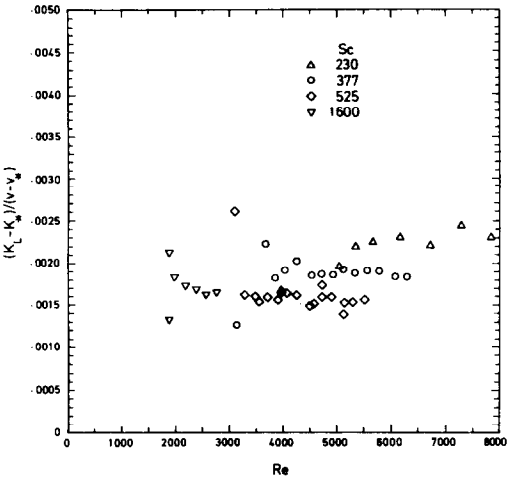

FIG. 9. $(K_L - K_*)/(v - v_*)$ vs Re for $Re > Re_*$.

His model was supported by data from Kishinevsky and Serebryansky [20], who generated their liquid-side turbulence with a submerged mechanical stirrer operating at very high speed (1700 r.p.m.). It is likely that Kishinevsky and Serebryansky's data lie well in the 'post-break' region, as evidenced by the very high stirring speed. For $K_L \gg K_*$ and $v \gg v_*$, equation (18) gives

$$St \simeq 0.0020 \quad (Re \gg Re_*), \tag{19}$$

which is in qualitative agreement with the results of ref. [20]. Note, however, that a body of data centered around the break region might (particularly when plotted on a log–log scale) suggest that K_L is proportional to v^n, where n is greater than unity. Our two-regime correlation is thus able, at least qualitatively, to reconcile the two seemingly conflicting classes of models: one broad class which advocates an $Sc^{-0.5}$ dependence and the other which suggests an independence of Sc. It should be noted, however, that the 'pre-break' region of our correlation has a linear dependence on v, rather than the $v^{1/2}$ dependence of Fortescue and Pearson [17] or the $v^{3/4}$ dependence of Lamont and Scott [18].

To summarize, our data can be correlated with the equations

$$St\,Sc^{0.5} \simeq 0.010 \pm 0.002 \quad (Re < Re_*) \tag{20}$$

$$St \simeq 0.002 + (0.01\,Sc^{-0.5} - 0.002)(Re_*/Re) \quad (Re > Re_*) \tag{21}$$

where

$$Re_*\,Sc^{0.4} = 3.5 \times 10^4. \tag{22}$$

Equation (21) results from substituting equations (20) and (22) into (18).

Note that up to this point, the velocity used to define St and Re is the value of *either* the horizontal or vertical fluctuating velocity components at the *centerline* of the test cell, extrapolated from the bulk to

the surface. The actual turbulence intensity decreases with radial distance. The *average* value of v over the free surface can be taken to be 90% of the centerline value of v extrapolated to the interface [6]. This implies that, if we base both St and Re on the *local r.m.s. velocity*, equations (20)–(22) become

$$St\,Sc^{0.5} \simeq 0.011 \pm 0.002 \quad (Re < Re_*) \tag{23}$$

$$St \simeq 0.0022 + (0.011\,Sc^{0.5} - 0.0022)(Re_*/Re) \quad (Re > Re_*) \tag{24}$$

where

$$Re_*\,Sc^{0.4} \simeq 3.2 \times 10^4. \tag{25}$$

Equations (23)–(25) are applicable for $500 < Re < 8000$ and $230 < Sc < 1600$.

5. DISCUSSION AND COMPARISON WITH PREVIOUS DATA

Equations (23)–(25) imply a linear dependence of the transfer coefficient on r.m.s. velocity at both pre-break and post-break conditions. The slopes are, however, different in the two regions. In the pre-break region, the slope is proportional to $Sc^{-0.5}$ and independent of macroscale. After the break, the slope depends on both Sc and Λ, but the dependence of both these parameters disappears at r.m.s. velocities much higher than the break value. We also note that a body of data in the neighborhood of the break may appear to show a faster than linear rise with r.m.s. velocity, and a different dependence on Sc and Λ.

In this section, we shall review some of the data available in the literature for consistency with our present correlation. We have selected only data for which at least rough estimates can be made of the r.m.s. velocity and length scale. Considering that these estimates are in most cases inaccurate, the comparisons presented here must be viewed only in broad terms, addressing issues of scaling and the existence of pre- and post-break regions rather than the exact values of the empirical coefficients in the correlating equations. Not included at all in these comparisons are thin-film gravitational flows, in which surface waviness and wave breaking often play significant roles [21–23], suggesting that v and Λ are insufficient to characterize the mass transfer mechanism.

Most of the previous attempts at correlating gas absorption data, or providing an analytical basis for the correlations (e.g. see the review in ref. [3]), have come up with a single equation of the form

$$St \equiv K_L/v = \text{constant}\ Sc^{-m}\ Re^{n}. \tag{26}$$

Three models, each based on its own simplified view of the turbulent transport process at the interface, seem to have taken particular hold in the earlier literature. One is the 'large-eddy' model [2, 17], with $m = 0.5$ and $n = +0.5$. The other is the 'small-eddy' model [18], with $m = 0.5$ and $n = -0.25$. The third is Levich's model, with $m = 0.5$ and $n = +0.5$. More recent data for channel flows have supported $m = 0.5$ and $n = 0$, for wind-induced flows (where this correlation can be justified with scaling arguments) as well as for cases with no shear applied at the interface (where there is no obvious theoretical justification for the applicability of this power-law form).

Two-regime behavior has been suggested previously by Theofanous *et al.* [4] and by McCready and Hanratty [24, 25], and has also been noted in experiments with highly wind-swept interfaces. Based on various literature data and on a belief that the large- and small-eddy models represent lower and higher Reynolds number turbulent flow limits, Theofanous *et al.* [4] postulated a break at $Re \approx 500$, with $K_L \sim v^{0.5}$ at lower Re and $K_L \sim v^{0.75}$ at higher Re. The break observed by McCready and Hanratty [24, 25] and those found in experiments with high wind-induced turbulence have different (unrelated) origins, and will be discussed separately elsewhere. Generally, they differed from our system in that turbulence in the liquid is induced by interfacial shear stress, imposed by a moving gaseous medium above.

Table 4 summarizes some comparisons with previous data, the selection criteria being that the Schmidt number be large, that both v and Λ be at least estimable, and that the interface be at least approximately flat. These data are discussed below.

5.1. *Open-channel flow*

Sonin *et al.* [3] have shown that the data of Krenkel and Orlob [26] and Eloubaidy *et al.* [27] (as referenced in Plate and Friedrich [28]) can be expressed approximately as shown in Table 4, if the Stanton number is based on the streamwise component of fluctuating velocity near the surface. This agrees in form with equation (23), but differs by a factor of two.

The largest v in these data sets was 0.04 m s^{-1}, and the largest channel depth was 0.145 m. Estimating Λ to be 1/10 the channel depth, we find that the maximum value of the break point parameter in these data sets is 7×10^3, which is a factor of five smaller than the value associated with the break (equation (25)). Apart from the factor of two difference in the coefficient, some of which may be attributable to our estimate of v, these data are thus consistent with our correlation.

5.2. *Grid-induced turbulence in open-channel flow*

Fortescue and Pearson [17] measured the transport coefficient in an open channel with a grid inserted to produce turbulence. They assumed that the turbulence at the interface was the same as that behind an infinite grid, as given by Batchelor and Townsend [29], and claimed good agreement with their 'large-eddy' model, which predicts that the transfer coefficient varied as the square-root of the r.m.s. velocity and the inverse square-root of the macroscale.

Fortescue and Pearson's paper [17] is important because it appears to clearly support the large-eddy model, from which one might infer that it contradicts our present correlation. A careful examination of the

Table 4. Comparison with previous data

Reference	Correlation†	Range of Sc or Pr	Equivalent $(Re\,Sc^{0.4})_{max}$	Type of flow
Krenkel and Orlob [26] Eloubaidy *et al.* [27]	$St\,Sc^{0.5} \simeq 0.020$ (a)	$Sc \simeq 500$	7×10^3	Flow down an inclined channel
Fortescue and Pearson [17]	$St\,Sc^{0.5} \simeq 0.01$ (d)	$Sc \simeq 570$	3×10^3	Grid-induced turbulence in an open channel flow
Isenogle [30]	$St\,Sc^{0.5} \simeq 0.017$ (b)	$150 < Sc < 1050$	1×10^4	Submerged oscillating grid
Ho [32]	$St\,Sc^{0.5} \simeq 0.016$ (a)	$Sc \sim 500$	3×10^3	
Kishinevsky and Serebryansky [20]	$St \simeq 0.005$ (d)	$300 < Sc < 600$	5×10^4 (H_2) 7×10^4 (O_2) 7×10^4 (N_2)	Submerged mechanical stirrer operating at 1700 r.p.m.

† The letter indicates the classification of our 'best estimate' of the uncertainty in the deduction of St from the given data. In most cases, the uncertainty comes from the estimation of v, which is classified as: (a) $\pm 25\%$; (b) $\pm 50\%$; (c) $\pm 100\%$; (d) $\pm 200\%$.

paper shows, however, that their data seem, in fact, to be quite consistent with our pre-break correlation, equation (23), which has a linear dependence on v. Figure 10 shows a re-drawing of Fortescue and Pearson's Fig. 12, which plots the mass transfer coefficient vs Reynolds number Re_{FP} for two of their grid configurations. (The units and zero are not shown on the ordinate of their Fig. 12, but can be deduced from their Fig. 14, which plots the same data on a logarithmic scale.) Their Reynolds number is defined as $Re_{FP} \equiv 4Uhw/v(w+2h)$, where U is the mean flow speed, h is the water depth, w is the channel width, and v is the liquid kinematic viscosity. Figure 10 demonstrates that the turbulent transport coefficient (for $Re_{FP} > 4000$) varied essentially in a linear form with U in Fortescue and Pearson's experiments. The r.m.s. velocity v was proportional to U in Fortescue and Pearson's experiments. The proportionality coefficient was not measured directly, however, and is in our view open to some question. Fortescue and Pearson evaluated it (see their equation (25)) using Batchelor and Townsend's [29] expression for turbulence produced downstream of 'infinite' grids. Based on this expression, one predicts an average v over their mass transfer test section of about

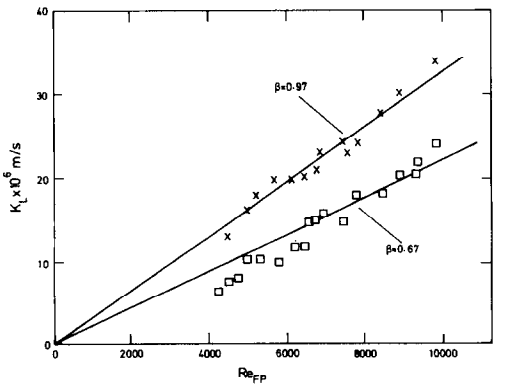

FIG. 10. Mass transfer coefficient, K_L (m s^{-1}), vs Reynolds number, Re_{FP}, for Fortescue and Pearson's data [17].

$v \approx 0.02U$ for one of their typical grid configurations. However, given the fact that their test section length was about 24 times the water depth, and that the test section was preceded by an equally long 'calming section', it seems likely that the turbulence resulting from the shear at the channel's bottom (and top, in the calming section) was at least as important as that produced by the grid.

In a fully developed turbulent channel flow, the shear-induced turbulence is $v \sim 0.1U$, i.e. significantly higher than grid-induced turbulence in the experiments of Fortescue and Pearson, but not necessarily overwhelmingly so. We may assume that $v = \beta U$, where in Fortescue and Pearson's experiments β was a coefficient of order 0.1 whose precise magnitude depended to some degree on the experimental conditions (grid configuration, entrance configuration, etc.). The two data sets in Fig. 10 can be fitted with our equation (23) with $\beta = 0.97$ and 0.67 respectively. These are reasonable figures and, as might be expected, the higher value of β is associated with the configuration where the grid was closer to the beginning of the test section.

Fortescue and Pearson's data lie well below the break point observed in our present correlation. With $\beta = 0.1$, and conservatively estimating Λ as equal to the water depth h, the maximum value of the break point parameter in Fortescue and Pearson's data is 3×10^3, which is an order of magnitude below our break point (equation (25)). It would appear, therefore, that Fortescue and Pearson's data are in fact consistent with our present correlation.

5.3. *Submerged oscillating grid*

The submerged oscillating grid has been used previously by a number of researchers to generate 'homogeneous' turbulence, which decays as the free surface is approached, much as in our own jet system. Isenogle [30], following up the work of Dickey *et al.* [31], made numerous measurements in such a system of both the horizontal and vertical r.m.s. velocities at various

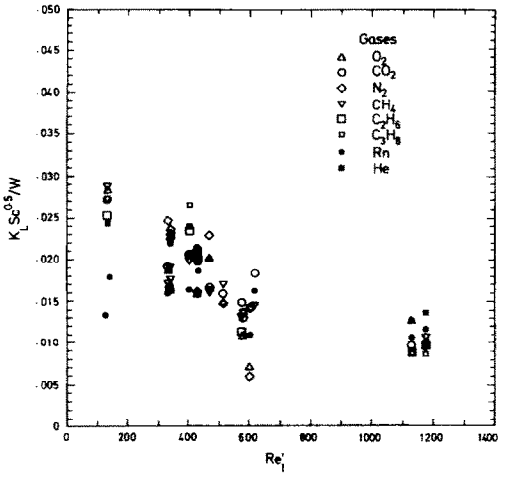

FIG. 11. $K_L\ Sc^{0.5}/W$ vs Re_I' for Isenogle's mass transfer data [30].

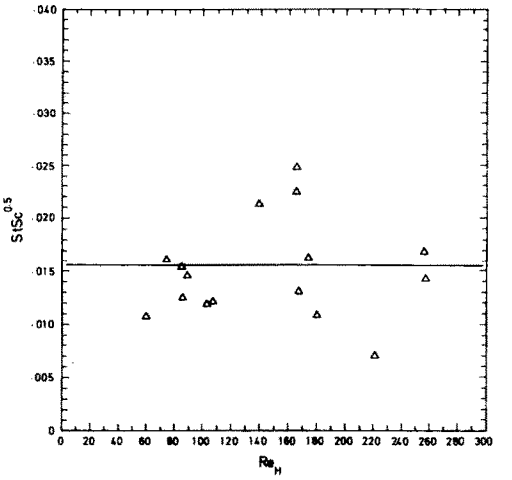

FIG. 12. $St\ Sc^{0.5}$ vs Re_H for Ho's mass transfer data [32].

depths beneath the interface and various operating conditions. He also made measurements of the integral length scale, Λ_I, defined as

$$\Lambda_I \equiv \int_0^{\infty} f(r)\,\mathrm{d}r \tag{27}$$

where

$$f(r) = \langle u(r_0)u(r_0+r)\rangle/\langle u^2(r_0)\rangle$$

u is the fluctuating velocity, r_0 is the reference location, r is the mean separation distance and $\langle\ \rangle$ is the ensemble average. This length is comparable with, but not exactly equal to, the turbulence macroscale Λ used in Brown *et al.* [6]. Using the absolute turbulent velocity $W \equiv \langle(u^2+v^2+w^2)^{0.5}\rangle$ and Λ_I extrapolated to the interface, we replotted Isenogle's mass transfer data in Fig. 11. $K_L Sc^{0.5}/W$ levels off to a value of about 0.01 when Re_I' ($\equiv W\Lambda_I/\nu$) exceeds about 600. If we assume that the total kinetic energy does not change significantly in the 'damped' layer next to the interface, then v, the r.m.s. velocity extrapolated from the bulk to the interface, can be written as $v \simeq W/3^{0.5}$, and Isenogle's data can be re-correlated as $K_L Sc^{0.5}/v \simeq 0.017$ for Re_I ($\equiv v\Lambda_I/\nu$) greater than 400, which agrees rather well with equation (23). For $Re_I < 400$, $K_L Sc^{0.5}/v$ shows some indication of rising above 0.017. The correlation as given in equation (23) was obtained for higher Re, mainly $8000 > Re > 500$. Note, however, that the rise at $Re_I < 400$ is quite different from the data of McCready and Hanratty [24, 25], who observed a decrease in K_L/v at $Re < 50$ for the case of turbulence induced by surface shear. In Isenogle's data, we find a maximum break point parameter of 1×10^4, which is smaller than the critical value associated with the break point, consistent with Isenogle's data being in the pre-break region.

Ho [32] has also used a submerged oscillating grid apparatus to measure the transfer of O_2 across a turbulent interface. Ho's apparatus was the same as that used by Brumley and Jirka [33], who reported that, provided one is not too close to the interface, the scaling relationship of Hopfinger and Toly [34],

$$v = 0.25 f s^{1.5} M^{0.5}/z' \tag{28}$$

$$\Lambda_{TH} = 0.1 z', \tag{29}$$

is a fairly good approximation of the velocity field. Here v is the r.m.s. horizontal or vertical velocity, Λ_{TH} is the macroscale, f is the grid frequency, s is the stroke amplitude, M is the mesh size of the grid, and z' is the distance from the virtual origin (which is close to the center of oscillation). Taking the r.m.s. velocity and length scale at the interface as given by equations (28) and (29), respectively, we reduced Ho's mass transfer data to the form $St\ Sc^{0.5}$ vs Re_H ($\equiv v\Lambda_{TH}/\nu$) as plotted in Fig. 12. Although there is some scatter in the plot, a mean value of $St\ Sc^{0.5} \simeq 0.016$ is obtained, independent of Re_H. This compares favorably with equation (23). For Ho's data, the maximum value of the break point parameter turns out to be 3×10^3, which is smaller than the critical value, consistent with our proposed correlation.

5.4. *Submerged high speed mechanical stirrer*

The only experiment that we are aware of which may be in the 'post-critical' region are those of Kishinevsky and Serebryansky [20]. Kishinevsky and Serebryansky used a high-speed submerged mechanical stirrer to generate turbulence in a cylindrical test cell. The stirring rate was kept constant at 1700 r.p.m. and mass transfer data were collected for three different gases, nitrogen, oxygen and hydrogen, at 20°C. In order to reduce their data to our form, we follow McManamey *et al.* [35] (see also ref. [36]) and write, for turbulence generated by a stirrer,

$$v \sim 0.55NL \tag{30}$$

$$\Lambda_M \sim 0.3L, \tag{31}$$

where v is the turbulence fluctuation near the interface, N is the stirring speed (revolutions per second), L is the length (tip to tip) of the stirrer blade, and Λ_M is the characteristic eddy dimension (macroscale). Using equations (30) and (31), we can restate Kishinevsky and Serebryansky's result as

$$St \sim 0.0045. \tag{32}$$

Equation (24) yields $St \simeq 0.0014$ for the three different gases. Except for the constant, which differs by a factor of about 3, the agreement is good, given the various approximations made. As to whether Kishinevsky and Serebryansky's data belong to the 'post-critical' region, the break point parameter turns out to have values well above the critical values (see Table 4).

6. CONCLUSIONS

An empirical correlation has been derived for high Schmidt number gas absorption into a shear-free, turbulent liquid interface. The correlation has the form

$$St\, Sc^{0.5} = 0.011 \quad (Re < Re_*) \tag{33}$$

$$St = 0.0022 + (0.011 Sc^{-0.5} - 0.0022)(Re_*/Re)$$

$$(Re > Re_*) \tag{34}$$

where $St \equiv K_L/v$ and $Re_* = 3.2 \times 10^4 Sc^{-0.4}$ is the break point parameter: a break occurs in the correlation when this parameter reaches the critical value of 3.2×10^4.

The correlation is based on data in the range $500 < Re < 8000$ and $230 < Sc < 1600$, where $Re = v\Lambda/\nu$ is the eddy Reynolds number. The correlation is in good agreement with much of the available data and although it is derived strictly from our own laboratory data, draws together several apparently disparate results in different studies.

At this point, we have no satisfactory model for the transfer process, and no physical explanation of why the break occurs. The break is definitely *not* associated with wave-breaking (the interface remained relatively flat with surface wave amplitudes of below a few millimeters for all our tests) or gas bubble entrainment into the liquid, which are implicated in the breaks observed with wind-driven interfaces.

We note that a correlation similar to equation (33), but with a 0.33 power dependence on the Prandtl number, has been obtained for the analogous condensation heat transfer process by Brown *et al.* [6] at *low* Prandtl numbers, $1 < Pr < 6$. Brown *et al.* used a similar system and similar turbulence intensities as in the present study, but observed no break point. This may be tentatively explained by the fact that, because of the low Prandtl numbers, the break point parameter was below the critical value in all of Brown *et al.*'s tests. However, not knowing the mechanism of the break, there is no reason to assume that the break point criterion would be identical at low and high Schmidt/Prandtl numbers.

Acknowledgements—This work partly supported by Grant NAG3-731 from NASA Lewis Research Center, and monitored by J. C. Ayolelott and D. M. DeFelice. One of us (B.C.K.) was supported by the Singapore government during this work.

REFERENCES

1. W. K. Lewis and W. G. Whitman, Principles of gas absorption, *Ind. Engng Chem.* **16,** 1215 (1924).
2. R. Higbie, The rate of absorption of a pure gas into a still liquid during short periods, *A.I.Ch.E. Jl* **25,** 122–131 (1935).
3. A. A. Sonin, M. A. Shimko and J. H. Chun, Vapor condensation onto a turbulent liquid—I. The steady condensation rate as a function of liquid side turbulence, *Int. J. Heat Mass Transfer* **29,** 1319–1332 (1986).
4. T. G. Theofanus, R. N. Houze and L. K. Brumfield, Turbulent mass transfer at free gas–liquid interfaces, with applications to open-channel, bubble and jet flows, *Int. J. Heat Mass Transfer* **19,** 613–624 (1976).
5. W. Brutsaert and G. H. Jirka (Editors), *Gas Transfer at Water Surfaces*. Reidel, Dordrecht (1984).
6. J. S. Brown, B. C. Khoo and A. A. Sonin, Rate correlation for condensation of pure vapor on turbulent, subcooled liquid, *Int. J. Heat Mass Transfer* **33,** 2001–2018 (1990).
7. E. A. Brignole and R. Echarte, Mass transfer in laminar liquid jets, *Chem. Engng Sci.* **36,** 695–703 (1981).
8. J. D. Cox and A. J. Head, Solubility of carbon dioxide in hydrofluoric acid solutions, *Trans. Faraday Soc.* **58,** 1839–1845 (1962).
9. H. S. Harned and R. Davis, The ionization constant of carbonic acid in water and solubility of carbon dioxide in water and aqueous salt solution, *J. Am. Chem. Soc.* **65,** 2030–2041 (1943).
10. B. C. Khoo, A numerical and experimental study of the scalar transport at a turbulent liquid free surface, Ph.D. Thesis, Massachusetts Institute of Technology, Cambridge, MA (1988).
11. L. Merlivat and L. Memery, Gas exchange across an air–water interface: experimental results and modelling of bubble contribution to transfer, *J. Geophys. Res.* **88,** No. C1, 707–724 (1983).
12. H. Broecker, J. Petermann and W. Siems, The influence of wind on CO_2-exchange in a wind-wave tunnel, including effects of monolayers, *J. Marine Res.* **36,** 595–610 (1978).
13. H. Broecker and W. Siems, The role of bubbles for gas transfer from water to air at higher windspeeds. In *Gas Transfer at Water Surfaces* (Edited by W. Brutsaert and G. H. Jirka), pp. 229–236. Reidel, Dordrecht (1984).
14. J. T. Davies, *Turbulence Phenomena*. Academic Press, New York (1972).
15. J. T. Davies, A. A. Kilner and G. A. Ratcliff, The effect of diffusivities and surface films on gas absorption, *Chem. Engng Sci.* **19,** 583–590 (1964).
16. M. A. Orridge, Gas absorption into turbulent streams of liquids, Ph.D. Thesis, University of Birmingham, U.K. (1970).
17. G. E. Fortescue and J. R. A. Pearson, On gas absorption into a turbulent liquid, *Chem. Engng Sci.* **22,** 1163–1176 (1967).
18. J. C. Lamont and D. S. Scott, An eddy cell model of mass transfer into the surface of a turbulent liquid, *A.I.Ch.E. Jl* **16,** 513–519 (1970).
19. M. Kh. Kishinevsky, Two approaches to the theoretical analysis of absorption processes, *J. Appl. Chem. U.S.S.R.* **28,** 881–886 (1955) [translation pagination].

20. M. Kh. Kishinevsky and V. T. Serebryansky, The mechanism of mass transfer at the gas–liquid interface with vigorous stirring, *J. Appl. Chem. U.S.S.R.* **29,** 29 33 (1956) [translation pagination].
21. K. J. Chu and A. E. Dukler, Statistical characteristics of thin, wavy films: II. Studies of the substrate and its wave structure, *A.I.Ch.E. Jl* **20,** 696–706 (1974).
22. K. J. Chu and A. E. Dukler, Statistical characteristics of thin, wavy films: III. Structure of the large waves and their resistance to gas flow, *A.I.Ch.E. Jl* **21,** 583–593 (1975).
23. N. Brauner and D. M. Maron, Characteristics of inclined thin films, waviness and the associated mass transfer, *Int. J. Heat Mass Transfer* **25,** 99–110 (1982).
24. M. J. McCready and T. J. Hanratty, Concentration fluctuation close to a gas–liquid interface, *A.I.Ch.E. Jl* **30,** 122–131 (1984).
25. M. J. McCready and T. J. Hanratty, A comparison of turbulent mass transfer at a gas–liquid and solid–liquid interface. In *Gas Transfer at Water Surfaces* (Edited by W. Brutsaert and G. H. Jirka), pp. 283–292. Reidel, Dordrecht (1984).
26. P. A. Krenkel and G. I. Orlob, Turbulent diffusion and the reaeration coefficient, *Trans. A.S.C.E.* **128,** 293–323 (1963).
27. A. F. Eloubaidy, E. J. Plate and J. Gessler, Wind waves and the reaeration coefficient in open channel flow, Report No. CER 69.70 AFE 2, Department of Civil Engineering, Colorado State University (1969).
28. E. J. Plate and R. Friedrich, Reaeration of open channel flow. In *Gas Transfer at Water Surfaces* (Edited by W. Brutsaert and G. H. Jirka), pp. 333–346. Reidel, Dordrecht (1984).
29. G. K. Batchelor and A. A. Townsend, *Proc. R. Soc.* **193A,** 539 (1948).
30. S. S. Isenogle, A laboratory study of gas transfer across an air–water interface, M. S. Thesis, University of Southern California, Los Angeles, CA (1985).
31. T. D. Dickey, B. Hartman, D. Hammond and E. Hurst, A laboratory technique for investigating the relationship between gas transfer and fluid turbulence. In *Gas Transfer at Water Surfaces* (Edited by W. Brutsaert and G. H. Jirka), pp. 93–100. Reidel, Dordrecht (1984).
32. A. W. K. Ho, A study of oxygen transfer at the air water interface of a grid agitated tank, M.S. Thesis, Cornell University, New York (1987).
33. B. H. Brumley and G. H. Jirka, Near surface turbulence in a grid stirred tank, *J. Fluid Mech.* **183,** 235–263 (1987).
34. E. J. Hopfinger and J. A. Toly, Spatially decaying turbulence and its relation to mixing across density interfaces, *J. Fluid Mech.* **78,** 155–175 (1976).
35. W. J. McManamey, J. T. Davis, J. M. Wollen and J. R. Coe, The influence of molecular diffusion on mass transfer between turbulent liquids, *Chem. Engng Sci.* **28,** 1061–1069 (1973).
36. J. T. Davies and F. J. Lozano, Turbulence characteristics and mass transfer at air–water interface, *A.I.Ch.E. Jl* **25,** 405–415 (1979).

FORMULE DE TRANSFERT D'UN SCALAIRE A TRAVERS LA SURFACE LIBRE D'UN LIQUIDE TURBULENT: UNE FORMULE A DEUX REGIMES POUR LES NOMBRES DE SCHMIDT ELEVES

Résumé—On établit une formule empirique pour l'absorption de gaz à l'interface turbulent d'un liquide. Cette formule est exprimée en fonction de l'intensité de la turbulence et de la macro-échelle du côté liquide et des propriétés du gaz et du solvant. Le coefficient de transfert augmente linéairement avec la moyenne quadratique de la vitesse fluctuante, jusqu'au point où le nombre de Reynolds atteint une valeur critique (dépendant du nombre de Schmidt). Aux vitesses plus élevées, il y a une croissance plus rapide. La pente de la région à faible nombre de Reynolds est proportionnelle à la racine carrée de la diffusivité; aux nombres de Reynolds plus élevés que le point de rupture, la pente devient indépendante de la diffusivité.

KORRELATION FÜR DIE FREIE OBERFLÄCHE EINER TURBULENTEN FLÜSSIGKEIT IN ZWEI BEREICHEN BEI HOHER SCHMIDT-ZAHL

Zusammenfassung—Aufgrund von Meßergebnissen wird eine Korrelation für die Gasabsorption an der Grenzfläche einer turbulenten und schubspannungsfreien Flüssigkeit entwickelt. Sie enthält die Turbulenzintensität der flüssigen Seite, die Abmessungen der flüssigen Seite und die Eigenschaften des diffundierenden Gases und Lösungsmittels. Der Transportkoeffizient nimmt linear mit der mittleren Geschwindigkeit bis zu einem Punkt zu, an dem die Wirbel-Reynolds-Zahl (abhängig von der Schmidt-Zahl) einen kritischen Wert erreicht. Bei höheren Geschwindigkeiten kommt es zu einem steileren linearen Anstieg. Die Neigung ist im Bereich kleiner Reynolds-Zahlen proportional zur Quadratwurzel der Temperaturleitfähigkeit; bei Reynolds-Zahlen weit oberhalb des Knickpunktes ist die Neigung von der Temperaturleitfähigkeit unabhängig.

ОБОБЩАЮЩАЯ ЗАВИСИМОСТЬ ДЛЯ СКАЛЯРА СКОРОСТИ НА ПОВЕРХНОСТИ ТУРБУЛЕНТНОЙ ЖИДКОСТИ ПРИ ОТСУТСТВИИ СДВИГА: ДВУХРЕЖИМНАЯ ЗАВИСИМОСТЬ ПРИ ВЫСОКИХ ЧИСЛАХ ШМИДТА

Аннотация—Получены экспериментальные характеристики в случае поглощения газа на границе турбулентной жидкости при отсутствии сдвига. Найдено соотношение, содержащее интенсивность турбулентиости со стороны жидкости, макромасштаб жидкости, а также свойства диффундирующего газа и растворителя. Коэффициент переноса линейно возрастает с увеличением среднеквадратичной скорости до точки, в которой турбулентное число Рейнольса достигает критического (зависящего от числа Шмидта) знажчения. При более высоких скоростях линейное увеличение коэффициента переноса происходит быстрее. Величина наклона в области низких чисел Рейнольдса пропорциональна квадратному корню из коэффициента диффузии; при числах Рейнольдса, значительно превышающих критическое значение, наклон перестает зависеть от коэффициента диффузии.